



UNIVERSITI PUTRA MALAYSIA

***ELECTROCHEMICAL PERFORMANCE OF FLEXIBLE POLYETHYLENE
TEREPHTHALATE-BASED DYE-SENSITIZED SOLAR CELL***

TAN JIAN HUA

FS 2017 76



**ELECTROCHEMICAL PERFORMANCE OF FLEXIBLE POLYETHYLENE
TEREPHTHALATE-BASED DYE-SENSITIZED SOLAR CELL**

By

TAN JIAN HUA

**Thesis Submitted to the School of Graduate Studies, Universiti Putra Malaysia, in
Fulfilment of the Requirement for the Degree in Master of Science**

June 2017

COPYRIGHT

All material contained within the thesis, including without limitation text, logos, icons, photographs and all other artwork, is copyright material of Universiti Putra Malaysia unless otherwise stated. Use may be made of any material contained within the thesis for non-commercial purposes from the copyright holder. Commercial use of material may only be made with the express, prior, written permission of Universiti Putra Malaysia.

Copyright © Universiti Putra Malaysia



Abstract of thesis presented to the Senate of Universiti Putra Malaysia in fulfilment of the requirement for the degree of Master of Science

ELECTROCHEMICAL PERFORMANCE OF FLEXIBLE POLYETHYLENE TEREPHTHALATE-BASED DYE-SENSITIZED SOLAR CELL

By

TAN JIAN HUA

June 2017

Chair: Janet Lim Hong Ngee, PhD
Faculty: Science

Our earth's natural resources are being depleted at an alarming rate. Green energy is now in greater demand than ever as our resources are being consumed faster than they can be replenished. Hence, solar energy, the best form and source of renewable energy, can fulfil the ever-increasing demand for more and more energy. Therefore, the invention of the 3rd generation solar cell, otherwise known as the dye-sensitized solar cell (DSSC), can meet this demand and help overcome the dependence on fossil fuels and the like. The DSSC is very effective and efficient as it can perform in low-light conditions. It is very cost efficient as well when compared to previous generations of solar cells. In the present study, indium tin oxide coated on polyethylene terephthalate (ITO/PET) was utilized as the flexible substrate for both the photoanode and the counter electrode in the dye-sensitized solar cell (DSSC). The main objective of this study was to find out the performance of DSSCs sintered at different temperatures during the fabrication process. The photoanode comprising of a layer of titanium dioxide on an ITO/PET substrate ($\text{TiO}_2/\text{ITO/PET}$) was prepared by mild sintering at 140, 150, 160, 170 and 180 °C. Secondly, the intention of this study was to find out the effect different photoanode active area sizes have on the performance of the DSSC which had the best performance among samples from the previous step. The active areas of the photoanodes were set at 1.0 cm², 0.25 cm², and 0.09 cm². The DSSC assembly is incomplete without a counter electrode. The counter electrode is made by binding the polypyrrole and graphene oxide onto an ITO/PET substrate (PPy/rGO/ITO/PET). It was prepared using electrodeposition and was used in place of platinum for the counter electrode. Lastly, the study set out to test whether the DSSC works when in a bent condition. A cyclic voltammetry analysis showed that electron charge transfer occurs on the sensitized photoanode sintered at temperatures ranging from 140 - 180 °C during the fabrication process. The photoanode samples exhibited two anodic potential peaks, the first ranging from 0.70 V to 0.74 V and the second from 1.0 V to 1.3 V. However, no cathodic potential peak was seen, thus indicating that the oxidized ruthenium dye (N719) molecules have a short lifespan. The photoanode sample sintered at 160 °C gave the best efficiency when compared to samples sintered at other temperatures. The same photoanode with an active area of 0.25 cm² displayed

the best performance with an open circuit voltage (V_{oc}) of 0.63 V, a short circuit current density (J_{sc}) of 3.0 mA cm^{-2} , and an efficiency (η) of 0.91% under 1 sun illumination (100 mW cm^{-2} , AM 1.5G). Last but not least, the ITO/PET-based DSSC continues to work when bent albeit at a reduced efficiency.



Abstrak tesis yang dikemukakan kepada Senat Universiti Putra Malaysia, sebagai memenuhi keperluan untuk ijazah Master Sains

**PRESTASI ELEKTROKIMIA FLEXIBEL POLITILENA TEREPHTHALATE
BERASAKAN SEL-SEL SOLAR PEWARNA SENSITIF (DSSC)**

Oleh

TAN JIAN HUA

Jun 2017

Pengerusi: Janet Lim Hong Ngee, PhD
Fakulti: Sains

Sejak kebelakangan ini, sumber-sumber semula jadi di seluruh dunia semakin berkurang. Maka, permintaan untuk sumber tenaga hijau menjadi hebat disebabkan oleh sumber-sumber semula jadi yang hilang lebih cepat daripada yang dihasilkan. Kini, sel solar pewarna sensitif (DSSC), iaitu sel solar generasi ketiga, telahpun menjadi tumpuan kepada kebanyakan pihak. Hal ini adalah kerana sel pewarna ini dapat mengatasi masalah kekurangan bahan api fosil. Selain itu, sel pewarna ini masih efektif dan cekap walaupun dalam suasana yang kurang bercahaya. Dalam kajian ini, indium tin oksida yang disalut ke atas polietilena terephthalate (ITO/PET) telah digunakan sebagai substrat fleksibel untuk fotoanod dan kaunter elektrod dalam sel solar pewarna sensitif (DSSC). Objektif utama kajian ini adalah untuk mengetahui prestasi fotoanod DSSC yang disediakan pada suhu-suhu yang berlainan. Lapisan fotoanod terdiri daripada titanium oksida yang bersalut pada kepingan ITO/PET ($\text{TiO}_2/\text{ITO}/\text{PET}$) yang telah disediakan melalui rawatan pembakaran pada suhu 140, 150, 160, 170 dan 180 °C. Selain itu, kajian ini bertujuan untuk mengkaji prestasi elektrokimia sel solar pewarna sensitive yang terbaik berdasarkan kawasan aktif fotoanod yang ditetapkan pada 1.0 cm^2 , 0.25 cm^2 , and 0.09 cm^2 . Penggabungan kaunter electrod dengan fotoanod amat penting. Oleh itu, polipirrol bercampur dengan graphene oksida (PPy/rGO/ITO/PET) telah disediakan melalui pengelektroenanapan untuk mengganti kaunter elektrod yang berdasarkan platinum. Analisis voltammetri kitaran (CV) menunjukkan pemindahan elektron berlaku pada $\text{TiO}_2/\text{ITO}/\text{PET}$ fotoanod yang disediakan pada suhu 140 – 180 °C. Setiap fotoanod mempamerkan dua puncak pengoksidaan, puncak pertama antara 0.70 V - 0.74 V dan puncak yang kedua pada 1.0 V - 1.3 V. Walau bagaimanapun, reaksi pengurangan tidak berlaku, disebabkan oleh jangka hayat molekul oksida pewarna ruthenium yang sangat pendek. Analisis menunjuk bahawa fotoanod yang dipanaskan pada suhu 160 °C mempunyai prestasi yang terbaik berbanding dengan sampel-sampel yang lain. Sampel yang dipanaskan pada suhu 160 °C dan yang mempunyai kawasan aktif fotoanod yang berukuran 0.25 cm^2 , memperolehi prestasi arus litar pintas (J_{sc}) sebanyak 3.0 mA cm^{-2} , voltan litar terbuka (V_{oc}) bernilai 0.63 V, dan kecekapan (η) sebanyak 0.91% di bawah pencahayaan satu matahari (100 mW cm^{-2} , AM 1.5 G).

Akhir sekali, substrat fleksibel ITO/PET masih berfungsi walaupun bengkok, tetapi prestasinya tidak secepat berbanding dengan sampel biasa (rata) yang lain.



ACKNOWLEDGEMENTS

I want to express my deepest gratitude and heartfelt thanks to my supervisor, Associate Professor Dr. Janet Lim Hong Ngee for her continuous support and guidance. Without her, I would not have been able to complete the research present in this thesis. I would also like to thank her for all the opportunities that she has given me over the last two years. I want to thank my co-supervisor, Dr. Shahrul Ainliah Binti Alang Ahmad for her tireless efforts and advice, and for making me see aspects of my research which I did not see before. I would also like to thank all my seniors and lab mates for all the help they have provided whenever I had any questions or doubts. I want to extend my special thanks to Chan Keng Fuong for his never-ending patience and assistance over the course of my master's degree. Last but not least, I want to thank my family for their endless love, understanding and support throughout the years and their dedication to the materialization of my dream. Without them, I know I would not be writing this today.

Thank you all so very much. Your kindness has changed my life for the better.

This thesis was submitted to the Senate of Universiti Putra Malaysia and has been accepted as fulfilment of the requirement for the degree in Master of Science. The members of the Supervisory Committee were as follows:

Janet Lim Hong Ngee, PhD

Associate Professor
Faculty of Science
Universiti Putra Malaysia
(Chairman)

Shahrul Ainliah Binti Alang Ahmad, PhD

Senior Lecturer
Faculty of Science
Universiti Putra Malaysia
(Member)

ROBIAH BINTI YUNUS, PhD

Professor and Dean
School of Graduate Studies
Universiti Putra Malaysia

Date:

Declaration by Members of Supervisory Committee

This is to confirm that:

- The research conducted and the writing of this thesis was under our supervision;
- Supervision responsibilities as stated in the Universiti Putra Malaysia (Graduate Studies) Rules 2003 (Revision 2012-2013) are adhered to.

Signature: _____

Name of
Chairman of
Supervisory
Committee:

Associate Professor Dr. Janet Lim Hong Ngee

Signature: _____

Name of
Member of
Supervisory
Committee:

Dr. Shahrul Ainliah Binti Alang Ahmad

TABLE OF CONTENTS

	Page
ABSTRACT	i
ABSTRAK	iii
ACKNOWLEDGEMENTS	v
APPROVAL	vi
DECLARATION	viii
LIST OF TABLES	xii
LIST OF FIGURES	xiii
LIST OF EQUATIONS	xv
LIST OF ABBREVIATIONS	xvi
 CHAPTER	
 1 INTRODUCTION	 1
1.1 Introduction	1
1.2 Background of the Study	1
1.2.1 Dye-Sensitized Solar Cells (DSSCs)	2
1.2.2 Photoanode of Dye-Sensitized Solar Cells	2
1.2.3 Counter Electrode	2
1.3 Problem Statement	4
1.4 Research Objectives	4
1.5 Scope of Study	5
 2 LITERATURE REVIEW	 6
2.1 Introduction	6
2.2 The Dye-Sensitized Solar Cell	8
2.2.1 Types of Photoactive Semiconductors	8
2.2.1.1 Titanium Dioxide (TiO ₂)	10
2.2.1.2 Zinc Oxide (ZnO)	11
2.2.2 Types of Substrates	12
Types of Dyes	13
Types of Electrolytes	15
2.2.4.1 Liquid Electrolytes	16
2.2.4.2 Solid-State Electrolytes	17
2.2.4.3 Quasi-Solid State Electrolytes	17
Types of Counter Electrodes	19
2.3 Conclusion	
 3 MATERIALS AND METHODS	 20
3.1 Materials	20
3.2 Treatment of the ITO/PET Film	20
3.3 Preparation of the Photoanode	20
3.4 Preparation of the Counter Electrode	22
3.4.1 Preparation of the Graphene Oxide (GO)	22
3.4.2 Binding of the PPy/rGO to the ITO/PET	22
3.5 Assembly of the Photoanode and the Counter Electrode	24

3.6	Characterizations	24
3.6.1	Tests Performed on the Dye-Sensitized Solar Cells (DSSCs)	24
3.6.2	Morphology Analysis	25
3.6.3	Elemental Analysis	25
4	RESULTS AND DISCUSSION	26
4.1	Morphology of the TiO ₂ /ITO/PET	26
4.2	Confirmation of Elements within the Counter Electrode	28
4.3	Electrochemical Studies of the TiO ₂ /ITO/PET	29
4.3.1	Redox Reaction of the N719 Dye Absorbed by the TiO ₂ /ITO/PET Photoanode	29
4.3.2	Power Conversion Efficiency (PCE) of the TiO ₂ /ITO/PET Photoanode	30
4.3.2.1	Prominent Effects of Sintering Temperature on DSSC Efficiency	30
4.3.2.2	Prominent Effects of Active Area Size on DSSC Efficiency	32
	Prominent Effects of Bending on DSSC Efficiency	33
4.3.3	Kinetic Charge Transfer within the TiO ₂ /ITO/PET DSSC	35
4.3.3.1	Prominent Effects of Sintering Temperature on Kinetic Charge Transfer	35
4.3.3.2	Prominent Effects of Active Area Size on Kinetic Charge Transfer	36
4.3.3.3	Prominent Effects Bending on Kinetic Charge Transfer	37
5	CONCLUSION AND RECOMMENDATIONS	39
5.1	Conclusion	39
5.2	Recommendations	41
	REFERENCES	42
	APPENDICES	48
	BIODATA OF STUDENT	61

LIST OF TABLES

Table		Page
1	Comparison of the physical properties of PEN and PET films	12
2	A summary of the preparation methods used to synthesize various Pt-free materials for use in counter electrodes	19
3	The anodic and cathodic peak potentials of the TiO ₂ /ITO/PET photoanodes sintered at different temperatures analyzed using cyclic voltammetry in a 0.10 M TBAPF ₆ / acetonitrile solution at a scan rate of 50 mV s ⁻¹	30
4	Photovoltaic performance of photoanodes sintered at different temperatures. Under 100 mW cm ⁻² illumination with an active area of 0.25 cm ²	32
5	Performance of different active area sizes under 100 mW cm ⁻² illumination	33
6	Comparison of the photovoltaic performance for flat and bent TiO ₂ /ITO/PET DSSCs under 100mW cm ⁻² illumination with an active area of 0.25 cm ²	34
7	Impedance spectra values for TiO ₂ /ITO/PET photoanode samples sintered at different temperatures. Measured under a forward bias set at -0.70 V in dark conditions.	36
8	Different active area sizes under 100 mW cm ⁻² illumination. Measured under a forward bias set at -0.70 V in dark conditions	37
9	Comparison of photovoltaic performance of flat and bent TiO ₂ /ITO/PET DSSC with an active area measuring 0.25 cm ² under 100mW cm ⁻² illumination	38
10	Summary of different TiO ₂ /ITO/PET photoanode fabrication techniques and their respective efficiencies when measured under 100 mW cm ⁻² illumination	39

LIST OF FIGURES

Figure		Page
1	Figure 1: (a) Structure of graphene nanoribbons with armchair edges (left) and zigzag edges (right); (b) the monolayer graphene and multilayer graphene (graphite), carbon nanotube and buckyball structures. Adapted from (Lloyd Hughes & Jeon, 2012).	3
2	The energy level and mechanism of a DSSC device. Adapted from (Berginc et al., 2007).	8
3	Energy band gap values of various semiconductors and their respective potentials measuring using a normal hydrogen electrode (NHE) as the reference. Adapted from (Gratzel, 2001).	9
4	FESEM images of the Titanium dioxide in (a) rutile and (b) anatase crystalline forms. Adapted from (Li et al., 2016).	10
5	SEM images of TiO ₂ /ITO/PET samples prepared at room temperature using different molar ratios of TTIP (a) 0.36 M and (b) 0.036 M of TTIP respectively. Adapted from (Zhang et al., 2006).	11
6	SEM images of the ZnO nanorod film (a) and ZnO nanotube film (b). Adapted from (Martinson et al., 2008).	12
7	Molecular Structures for polypyridyl ruthenium complexes sensitizer (a) N3 (cis-Bis (thiocyanato)-bis(2,2'-bipyridyl-4,4'-dicarboxylic acid)-ruthenium (II)); (b) N712 (Tetra(tetrabutylammonium)[cis-di(thiocyanato)-bis(2,2'-bipyridyl-4,4'-dicarboxylic acid)-ruthenium (II)]); (c) N719 (bis(tetrabutylammonium)[cis-di(thiocyanato)-bis(2,2'-bipyridyl-4-carboxylate-4'-carboxylic acid)-ruthenium (II)]); the binding modes of carboxylate group to TiO ₂ (d) bidentate bridging ligand (e) bidentate chelating ligand. Adapted from (Lee et al., 2010).	14
8	(a) Molecular structure of redox dyes SM371 and SM315 featuring porphyrin cores. Adapted from (Mathew et al., 2014) and (b) The electron transfer process from the metal-organic sensitizer to the semiconductor in the context of a DSSC. Adapted from (Mishra et al., 2009).	15
9	Chemical structure of poly(N-alkyl-4-pyridine) iodide (PNR4VPI) and N-alkyl-4-vinylpyridine iodide (NRPI). Adapted from (Wu et al., 2008).	16
10	Scanning electron microscope images of thermosetting gel electrolytes created using PEGs with different molecular weights (a) low PAA-PEG 400 (b) PAA-PEG-20000. Adapted from (Wu et al., 2007).	17
11	The photoanode fabrication process.	21
12	The counter electrode fabrication process.	23
13	Diagram of the assembled DSSC (a) virtual representation; (b) photograph of the actual sample.	24
14	FESEM images of the TiO ₂ /ITO/PET nanoparticles from the sample sintered at a temperature of 160 °C for 1 h (a) 20,000x magnification; (b) 80,000x magnification, and (c) EDX spectrum	27

	of sintered TiO ₂ /ITO/PET photoanode.	
15	Raman spectra of (a) ITO/PET; (b) PPy/ITO/PET, and (c) PPy/rGO/ITO/PET.	28
16	Cyclic voltammograms of the TiO ₂ /ITO/PET photoanodes measured in a 0.10 M TBAPF ₆ /acetonitrile solution at a scan rate of 50 mV s ⁻¹ (a) dye-sensitized and non-sensitized photoanodes sintered at 160 °C; b) dye-sensitized photoanodes sintered at different temperatures.	30
17	(a) Current density-photovoltage curves; (b) Power-voltage curves of the TiO ₂ /ITO/PET photoanodes sintered at different temperatures for 1h. Under 100 mW cm ⁻² illumination with an active area of 0.25 cm ² .	31
18	(a) Current density-photovoltage curves; (b) Power-voltage curves of the TiO ₂ /ITO/PET photoanode with different active area sizes. All samples sintered at 160 °C for 1h.	32
19	TiO ₂ /ITO/PET photoanodes with active areas measuring (a) 1.0 cm ² ; (b) 0.25 cm ² and (c) 0.090 cm ² respectively.	33
20	(a) Current density-photovoltage curves; (b) Power-voltage curves of the TiO ₂ /ITO/PET photoanode sintered at 160 °C for 1h in flat and bent conditions.	34
21	(a) Nyquist plot and (b) Bode phase plot for dye-sensitized TiO ₂ /ITO/PET photoanodes sintered at different temperatures for 1h and measured under a forward bias set at -0.70 V in dark conditions.	36
22	(a) Nyquist plot and (d) Bode phase plot for dye-sensitized TiO ₂ /ITO/PET photoanodes with different active area sizes sintered at a temperature of 160 °C for 1h and measured under a forward bias set at -0.70 V in dark conditions.	37
23	(a) Nyquist plot and (d) Bode phase plot for the DSSCs in flat and bent conditions.	38
24	The images of the assembled DSSC in (a) flat and (b) bent conditions.	38

LIST OF EQUATIONS

Equation	Page
1 $P_{\max} = J_{\max} \times V_{\max}$	34
2 $FF = (J_{\max} \times V_{\max}) / (J_{sc} \times V_{oc})$	34
3 $\eta = P_{\max} / P_{in} = J_{sc} \times V_{oc} \times FF / P_{in}$	34
4 $\tau_r = 1 / (2 \times \pi \times f)$	35



LIST OF ABBREVIATIONS

TiO ₂	Titanium dioxide
ZnO	Zinc oxide
ZnONS	Zinc oxide nanosheets
ZnONTs	Zinc oxide nanotubes
CBD	Chemical bath deposition
NHE	Normal Hydrogen Electrode
I _{max}	Current at maximum power
P _{max}	Maximum power input
V _{max}	Voltage at maximum power
P _{in}	Incident photon flux
J _{sc}	Short-circuit current density
V _{oc}	Open-circuit voltage
FF	Fill factor
η / (PCE)	Solar energy power conversion efficiency
TCO	Transparent conductive oxide
ITO	Indium tin oxide
FTO	Fluorine-doped tin oxide
PET	Polyethylene terephthalate
PEN	Polyethylene naphthalate
EDLC	Electric double layer capacitor
LSV	Linear Sweep voltammetry
CV	Cyclic voltammetry
EIS	Electrochemical impedance spectra
R _{ct}	Charge-transfer resistance
HOMO	Highest occupied molecular orbital
LUMO	Lowest unoccupied molecular orbital
TTIP	Titanium isopropoxide
H ₂ SO ₄	Sulphuric acid
HCl	Hydrochloric acid
KMnO ₄	Potassium Permanganate
H ₂ O ₂	Hydrogen Peroxide

NapTS	Toluene-4-sulfonic acid sodium salt
GO	Graphene oxide
rGO	Reduced graphene oxide
TBAPF ₆	Tetra-n-butylammonium hexafluorophosphate
DSSC	Dye-sensitized solar cell
SCE	Saturated Calomel Electrode
PEDOT	Poly(3,4-ethylenedioxythiophene)
PPy	Polypyrrole
PANI	Polyaniline
PMMA	Polymethyl methacrylate
N3	<i>Cis</i> -Bis(thiocyanato)-bis(2,2'-bipyridyl-4,4'-dicarboxylic acid)-ruthenium (II)
N712	(Tetra(tetrabutylammonium)[<i>cis</i> -di(thiocyanato)-bis(2,2'-bipyridyl-4,4'-dicarboxylic acid)-ruthenium (II)])
N719	<i>Bis</i> (tetrabutylammonium)[<i>cis</i> -di(thiocyanato)-bis(2,2'-bipyridyl-4-carboxylate-4'-carboxylic acid)-ruthenium (II)]
UV	Ultraviolet
WF	Work function
PAA-PEG	Poly(acrylic acid)-(ethylene glycol)
PNR4VPI	Poly(<i>N</i> -alkyl-4-pyridine) iodide
NR'PI	<i>N</i> -alkyl pyridine iodide
NRPI	<i>N</i> -alkyl-4-vinylpyridine iodide
Fc/Fc ⁺	Ferrocene/ferrocenium
KI	Potassium Iodide
r.t.p	Room temperature (average of 23 °C)
τ _r	Lifespan of electrons
CB	Conduction band
AM 1.5 G	Air Mass 1.5 Global
I ⁻	Iodide ion
I ₃ ⁻	Triiodide ion
CNTs	Carbon nanotubes
NP	Nanoparticles
GNS	Graphene nanosheets
SnO ₂	Tin dioxide

CdTe	Cadmium telluride
WO ₃	Tungsten trioxide
CdS	Cadmium sulfide
1D	One dimension
Ti	Titanium
Ru	Ruthenium
COOH	Carboxylic acid
COO ⁻	Carboxylate group
H	Hydrogen
CE	Counter Electrode
Pt	Platinum
AC	Activated carbon
N-GF	Nitrogen-doped graphene foams
FESEM	Field emission scanning electron microscope
Z _n	Nerst Diffusion Impedance
f	Frequency

CHAPTER 1

INTRODUCTION

1.1 Introduction

In recent years, communities around the world have been concerned about the depletion of natural resources and their impact on the environment such as air pollution, water pollution and global warming. Therefore, renewable energy is now in greater demand as an alternative source of energy. Renewable energy such as solar, wind, tidal, and the like has been widely studied. More attention has been paid to solar energy due to its similarity to photosynthesis. The dye-sensitized solar cell (DSSC), a third generation solar energy device unlike those from previous generations, is not silicon based. The advantages of the dye-sensitized solar cell are its cost effectiveness, low-light performance and ease of production and handling (Ng *et al.*, 2015) This system provides an alternative method of generating electrical energy from solar energy.

In this study, the researcher will discuss the findings on the efficiency of the electron charge transfer on an indium doped tin oxide coated polyethylene terephthalate (ITO/PET) based substrate in a dye-sensitized solar cell. These performance findings are based on the variation of temperatures the photoanode was fabricated at, the different active area sizes of the photoanode and the flexible DSSC when bent.

1.2 Background of the Study

1.2.1 Dye-Sensitized Solar Cells (DSSCs)

Basically, the DSSC is comprised of two components, the photoanode and the counter electrode. The processes that take place in the photoanode are the photo-excitation of dye molecules upon irradiation and the photo-injection of electrons into the conduction band of the TiO_2 . The counter electrode works as the charge reservoir, and also functions as the site for the redox couple reaction of triiodide and iodide ions, as well as dye regeneration.

The underlying mechanism of the dye-sensitized solar cell begins with the incidence of photon energy. The ruthenium dye molecules release electrons upon excitation from the required photon wavelength, thus initiating the transfer of electrons from the highest occupied molecular orbital (HOMO) to the lowest unoccupied molecular orbital (LUMO). The excited electrons are promoted to the conduction band (CB) of the semiconductor oxide. The electrons are then transferred through an external circuit, eventually reaching the counter electrode. The complex system is completed through

the occurrence of a redox reaction as the iodide ion (I^-) donates an electron to the ruthenium dye on the anode and the oxidized iodide ion in the electrolyte is reduced to a triiodide (I_3^-) on the cathode (Caramori *et al.*, 2010; Pandikumar *et al.*, 2016; Zhang *et al.*, 2013).

1.2.2 Photoanode of Dye-Sensitized Solar Cells

To meet the demand for a portable DSSC, plastic substrates have been employed as an alternative to glass due to their light-weight and flexibility for mobile electronic devices (Chiu *et al.*, 2011; Zhang *et al.*, 2013). The use of conductive polymer substrates such as polyethylene terephthalate (PET) in DSSC devices has been widely studied because of its low-cost production, high impact resistance, ease of preparation and flexibility (Devi & Kavitha, 2016). The selection of the transparent conductive oxide substrate (TCO) is crucial because the sheet resistance of TCO electrodes highly affects transmittance and photocurrent density (Zhang *et al.*, 2013). In addition, the photovoltaic performance also depends on the structure and morphology of the semiconductor oxide film. The most common material used as a semiconductor is titanium dioxide (TiO_2) as it exhibits the lowest energy band gap of 3.2 eV (Gong *et al.*, 2012). Generally, TiO_2 performs better due to its microspherical structure that enables excellent electron transfer and accelerates the injection of electrons from the ruthenium dye to the TiO_2 film (Mikula *et al.*, 2015). The TiO_2 semiconductor also exists in different forms. For our purpose, the best form is the rutile form, as it is the most stable and chemically reactive form when compared to anatase and brookite forms. Nevertheless, the nanocrystalline structure of the TiO_2 is crucial in determining the amount of dye that can be absorbed during immersion and the extent to which screening effects hinder the photoexcitation process (Chen & Mao, 2007). The smaller surface area of the rutile TiO_2 absorbs less dye than an anatase TiO_2 (Liu & Aydil, 2009). As such, the method of synthesizing the photoanode is imperative in determining the photovoltaic performance of the DSSC. However, the use of plastic substrates presents a problem during the preparation process as they cannot withstand being heated to a temperature higher than 150 °C (Vivero-Escoto *et al.*, 2012). In order to fabricate a DSSC using a low-temperature process, a series of methods has been studied such as isostatic high-pressure pressing (Weerasinghe *et al.*, 2012), hot-pressing (Ezaka *et al.*, 2013), light pressure mechanical rolling (Yun *et al.*, 2016), hydrothermal method (Wu *et al.*, 2011), screen printing (Liu & Aydil, 2009), electrophoretic (Zhao *et al.*, 2009) and ultraviolet treatment (Zeng *et al.*, 2010).

1.2.3 Counter Electrode

The conventional platinum counter electrode is replaced with polypyrrole/ reduced graphene oxide (PPy/rGO). Pyrrole (Py) is a conductive polymer that has the ability to store huge amounts of charge and has great power conversion efficiency (Weerasinghe *et al.*, 2013). The choice to use graphene is due to its outstanding electric conductivity. Graphene exists as a single layer atomic structure consisting of pristine carbon atoms interconnected in a two-dimensionally arranged honeycomb lattice via the sp^2 molecular bond. The study of graphene has revealed many astonishing discoveries

particularly in relation to optical, electrical, thermal and mechanical applications due to its remarkable properties (Zubir *et al.*, 2015). The arrangement of carbon on the graphene layer can be seen in figure 1 (a), either in a zigzag or armchair arrangement (Gusynin *et al.*, 2008). The array of carbon atoms in a straight cut along the outer row of a hexagon produces a zigzag edge. When the edges go through the middle of the hexagon at an angle of 30° it is known as an armchair arrangement. Figure 1 (b) shows the various possible shapes of graphene such as monolayer graphene, multilayer graphene (graphite layer), carbon nanotubes (CNTs) and buckyball (Lloyd Hughes & Jeon, 2012). Basically, graphene can be found in reduced graphene oxide (rGO) and graphene oxide (GO) forms. The combination of pyrrole and graphene oxide synergistically improve the performance of the counter electrode (Lim *et al.*, 2014).

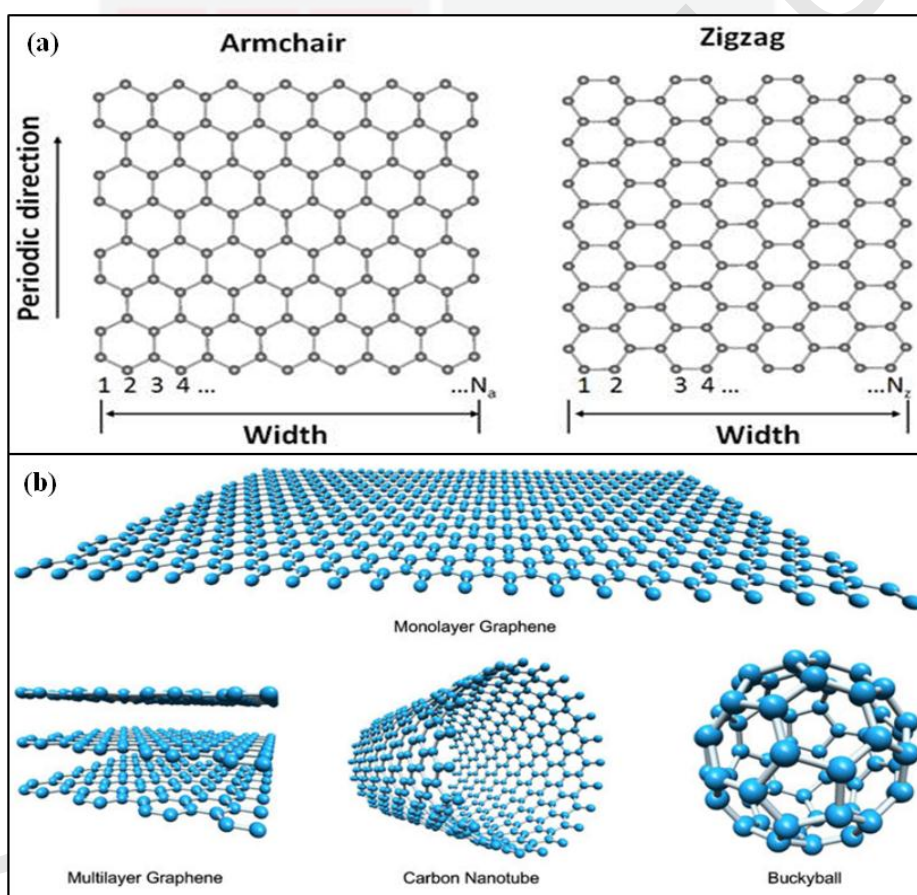


Figure 1: (a) Structure of graphene nanoribbons with armchair edges (left) and zigzag edges (right); (b) the monolayer graphene and multilayer graphene (graphite), carbon nanotube and buckyball structures. Adapted from (Lloyd Hughes & Jeon, 2012).

1.3 Problem Statement

Conventional solar panel technology used today is a great way to tap into the seemingly endless source of clean energy available to us from our sun. However, it is far from perfect and decades of research have been dedicated to its advancement. Common solar panels available today use a rigid glass substrate, which greatly limits its range of potential applications. They are heavy, fragile, and have low portability. Apart from that, they are also expensive to fabricate due to the large quantities of platinum required for the fabrication of the counter electrode. This research aims to circumvent these restrictions and limitations through the development of a flexible and lightweight solar cell which is also cost efficient. Weight and flexibility are important factors to consider when one wishes to add solar power capabilities to a product. For example, if one was to design a hybrid car that could harvest light energy to power the fuel cells within the vehicle, the weight of the solar panels would be an important consideration in the design process. If the panels are too heavy, the power generated from the solar panels would not be sufficient to warrant its implementation. If the cost of implementing the solar panels into the vehicle is too high, it would not make economic sense for the consumer. This is where a lightweight and flexible solar cell would be ideal. Application of the solar cell would be relatively easy as the solar cell would be able to bend to fit the shape of the vehicle. Being lightweight, it would not be a significant burden on the vehicle, thus preserving the performance and handling characteristics of the vehicle. The cost of production is also significantly lower than the conventional solar cell due to the lower cost of the raw materials required and a much simpler manufacturing process. This would make it an ideal candidate for adding solar power capabilities to the automotive and aerospace industry, or for emergency use by individuals in remote locations.

1.4 Objectives

General Objective

The main objective of this study is to gather electrochemical performance data on the $\text{TiO}_2/\text{ITO}/\text{PET}$ photoanode and the $\text{PPy}/\text{rGO}/\text{ITO}/\text{PET}$ counter electrode and how they perform together as a DSSC.

Specific Objectives

1. To study the performance of photoanodes sintered at various temperatures.
2. To study the effect different photoanode active area sizes have on the performance of the DSSC.
3. To study the performance of the DSSC when it is in a bent state.

1.5 Scope of Study

The scope of this research covers the performance of photoanodes sintered at various temperatures during fabrication, the performance different photoanode active area sizes have on the efficiency of the DSSC, and lastly to test how the DSSC performs when bent.

For this study, the researcher sintered the TiO_2 paste onto the ITO/PET substrate at 140 °C, 150 °C, 160 °C, 170 °C, and 180 °C. The researcher then tested them to find the best performing sample. The sample which gave the best results was the photoanode sintered at 160 °C. The researcher then made fresh samples of varying sizes sintered at 160 °C to measure the most efficient active area size. The active area sizes used for this measurement were 1.0 cm², 0.25 cm² and 0.090 cm². To test whether the DSSC works when bent, the DSSC was held at an angle of about 60° using paper clips.

Cyclic voltammetry, linear sweep voltammetry and impedance spectra analysis were carried out on the samples using a potentiostat machine (VersaSTAT Potentiostat Galvanostat from Princeton Applied Research). The morphology of the TiO_2 /ITO/PET photoanode was observed using a field emission scanning electron microscope (FEI Quanta SEM Model 400F). The materials in the photoanode sample were verified via energy dispersion X-ray spectroscopy (EDX) using the same FESEM model. The counter electrode was verified using Raman spectroscopy.



REFERENCES

- Ahn, H. J., Kim, I. H., Yoon, J. C., Kim, S. I., & Jang, J. H. (2014). p-Doped three-dimensional graphene nano-networks superior to platinum as a counter electrode for dye-sensitized solar cells. *Chemical communications*, 50(19), 2412-2415.
- Ali, M., Ibrahim, K., Hamad, O. S., Eisa, M., Faraj, M., & Azhari, F. (2011). Deposited indium tin oxide (ITO) thin films by dc-magnetron sputtering on polyethylene terephthalate substrate (PET). *Rom. J. Phys.*, 56(5-6), 730-741.
- Balint, R., Cassidy, N. J., & Cartmell, S. H. (2014). Conductive polymers: towards a smart biomaterial for tissue engineering. *Acta biomaterialia*, 10(6), 2341-2353.
- Balraju, P., Suresh, P., Kumar, M., Roy, M., & Sharma, G. (2009). Effect of counter electrode, thickness and sintering temperature of TiO₂ electrode and TBP addition in electrolyte on photovoltaic performance of dye sensitized solar cell using pyronine G (PYR) dye. *Journal of Photochemistry and Photobiology A: chemistry*, 206(1), 53-63.
- Berginc, M., Krašovec, U. O., Jankovec, M., & Topič, M. (2007). The effect of temperature on the performance of dye-sensitized solar cells based on a propyl-methyl-imidazolium iodide electrolyte. *Solar Energy Materials and Solar Cells*, 91(9), 821-828.
- Bertoluzzi, L., Lopez Varo, P., Tejada, J. A. J., & Bisquert, J. (2016). Charge transfer processes at the semiconductor/electrolyte interface for solar fuel production: insight from impedance spectroscopy. *Journal of Materials Chemistry A*, 4(8), 2873-2879.
- Biancardo, M., West, K., & Krebs, F. C. (2006). Optimizations of large area quasi-solid-state dye-sensitized solar cells. *Solar Energy Materials and Solar Cells*, 90(16), 2575-2588.
- Caramori, S., Cristino, V., Boaretto, R., Argazzi, R., Bignozzi, C. A., & Di Carlo, A. (2010). New Components for dye-sensitized solar cells. *International Journal of Photoenergy*, 2010, 1-16.
- Chee, W. K., Lim, H. N., & Huang, N. M. (2015). Electrochemical properties of free-standing polypyrrole/graphene oxide/zinc oxide flexible supercapacitor. *International Journal of Energy Research*, 39(1), 111-119.
- Chen, X., & Mao, S. S. (2007). Titanium dioxide nanomaterials: synthesis, properties, modifications, and applications. *Chem. Rev.*, 107(7), 2891-2959.
- Cheng, Y. T., Ho, J. J., Wang, C. K., Lee, W., Lu, C. C., Yau, B. S., Nain, J. L., Chang, S. H., Chang, C. C., & Wang, K. L. (2010). Improvement of organic solar cells by flexible substrate and ITO surface treatments. *Applied surface science*, 256(24), 7606-7611.
- Chiu, W.-H., Lee, K.-M., & Hsieh, W.-F. (2011). High efficiency flexible dye-sensitized solar cells by multiple electrophoretic depositions. *Journal of Power Sources*, 196(7), 3683-3687.
- Dai, H., Wang, N., Wang, D., Ma, H., & Lin, M. (2016). An electrochemical sensor based on phytic acid functionalized polypyrrole/graphene oxide nanocomposites for simultaneous determination of Cd (II) and Pb (II). *Chemical Engineering Journal*, 299, 150-155.

- De la Fuente Salas, I. M., Sudhakar, Y., & Selvakumar, M. (2014). High performance of symmetrical supercapacitor based on multilayer films of graphene oxide/polypyrrole electrodes. *Applied surface science*, 296, 195-203.
- Devi, L. G., & Kavitha, R. (2016). A review on plasmonic metal-TiO₂ composite for generation, trapping, storing and dynamic vectorial transfer of photogenerated electrons across the Schottky junction in a photocatalytic system. *Applied surface science*, 360, 601-622.
- Durr, M., Schmid, A., Obermaier, M., Rosselli, S., Yasuda, A., & Nelles, G. (2005). Low-temperature fabrication of dye-sensitized solar cells by transfer of composite porous layers. *Nature materials*, 4(8), 607-611. doi: 10.1038/nmat1433
- Eeu, Y. C., Lim, H. N., Lim, Y. S., Zakarya, S. A., & Huang, N. M. (2013). Electrodeposition of polypyrrole/reduced graphene oxide/iron oxide nanocomposite as supercapacitor electrode material. *Journal of Nanomaterials*, 2013, 157.
- Erten Ela, S., Yilmaz, M. D., Icli, B., Dede, Y., Icli, S., & Akkaya, E. U. (2008). A panchromatic boradiazaindacene (BODIPY) sensitizer for dye-sensitized solar cells. *Organic letters*, 10(15), 3299-3302.
- Ezaka, K., Yamamura, T., Yasufuku, T., Kishi, N., & Soga, T. (2013). Low-temperature Fabrication of Dye-sensitized Solar Cells on Plastic Films by Hot-pressing Method. *Chemistry Letters*, 42(10), 1263-1264.
- Fan, L. Q., Liu, G. J., Wu, J. H., Liu, L., Lin, J. M., & Wei, Y. L. (2014). Asymmetric supercapacitor based on graphene oxide/polypyrrole composite and activated carbon electrodes. *Electrochimica Acta*, 137, 26-33.
- Fu, N., Huang, C., Liu, Y., Li, X., Lu, W., Zhou, L., Peng, F., Liu, Y., & Huang, H. (2015). Organic-free anatase TiO₂ paste for efficient plastic dye-sensitized solar cells and low temperature processed perovskite solar cells. *ACS Applied Materials & Interfaces*, 7(34), 19431-19438.
- Gong, J., Liang, J., & Sumathy, K. (2012). Review on dye-sensitized solar cells (DSSCs): fundamental concepts and novel materials. *Renewable and Sustainable Energy Reviews*, 16(8), 5848-5860.
- Gratzel, M. (2001). Photoelectrochemical cells. *Nature*, 414(6861), 338-344. doi: 10.1038/35104607
- Gusynin, V., Miransky, V., Sharapov, S., & Shovkovy, I. (2008). Edge states in quantum Hall effect in graphene (Review Article). *Low Temperature Physics*, 34(10), 778-789.
- Hagfeldt, A., Boschloo, G., Sun, L., Kloo, L., & Pettersson, H. (2010). Dye-sensitized solar cells. *Chemical reviews*, 110(11), 6595-6663.
- Hegazy, A., Kinadjian, N., Sadeghimakki, B., Sivoththaman, S., Allam, N. K., & Prouzet, E. (2016). TiO₂ nanoparticles optimized for photoanodes tested in large area Dye-sensitized solar cells (DSSC). *Solar Energy Materials and Solar Cells*, 153, 108-116.
- Henderson, M. A. (2011). A surface science perspective on photocatalysis. *Surface Science Reports*, 66(6), 185-297.
- Hoshikawa, T., Yamada, M., Kikuchi, R., & Eguchi, K. (2005). Impedance analysis of internal resistance affecting the photoelectrochemical performance of dye-sensitized solar cells. *Journal of the Electrochemical Society*, 152(2), E68-E73.
- Hug, H., Bader, M., Mair, P., & Glatzel, T. (2014). Biophotovoltaics: Natural pigments in dye-sensitized solar cells. *Applied Energy*, 115, 216-225.

- Hung, I., & Bhattacharjee, R. (2016). Effect of Photoanode Design on the Photoelectrochemical Performance of Dye-Sensitized Solar Cells Based on SnO₂ Nanocomposite. *Energies*, 9(8), 641.
- Kapilashrami, M., Zhang, Y., Liu, Y.-S., Hagfeldt, A., & Guo, J. (2014). Probing the optical property and electronic structure of TiO₂ nanomaterials for renewable energy applications. *Chemical reviews*, 114(19), 9662-9707.
- Kim, H. S., Mora Sero, I., Gonzalez Pedro, V., Fabregat Santiago, F., Juarez Perez, E. J., Park, N. G., & Bisquert, J. (2013). Mechanism of carrier accumulation in perovskite thin-absorber solar cells. *Nature Communications*, 4, 2242.
- Kumar, S. G., & Rao, K. K. (2017). Comparison of modification strategies towards enhanced charge carrier separation and photocatalytic degradation activity of metal oxide semiconductors (TiO₂, WO₃ and ZnO). *Applied surface science*, 391, 124-148.
- Lai, Y. H., Lin, C. Y., Chen, H. W., Chen, J. G., Kung, C. W., Vittal, R., & Ho, K. C. (2010). Fabrication of a ZnO film with a mosaic structure for a high efficient dye-sensitized solar cell. *Journal of Materials Chemistry*, 20(42), 9379.
- Lee, K. E., Gomez, M. A., Elouatik, S., & Demopoulos, G. P. (2010). Further understanding of the adsorption mechanism of N719 sensitizer on anatase TiO₂ films for DSSC applications using vibrational spectroscopy and confocal Raman imaging. *Langmuir*, 26(12), 9575-9583.
- Lee, K. S., Lee, Y., Lee, J. Y., Ahn, J. H., & Park, J. H. (2012). Flexible and Platinum-Free Dye-Sensitized Solar Cells with Conducting-Polymer-Coated Graphene Counter Electrodes. *ChemSusChem*, 5(2), 379-382.
- Li, X., Zhang, C., & Meng, T. (2016). Synergistic effects from graphene oxide nanosheets and TiO₂ hierarchical structures enable robust and resilient electrodes for high-performance lithium-ion batteries. *RSC Adv.*, 6(6), 4321-4328.
- Liao, J. Y., Lei, B. X., Chen, H. Y., Kuang, D. B., & Su, C. Y. (2012). Oriented hierarchical single crystalline anatase TiO₂ nanowire arrays on Ti-foil substrate for efficient flexible dye-sensitized solar cells. *Energy & Environmental Science*, 5(2), 5750-5757.
- Lim, S. P., Huang, N. M., Lim, H. N., & Mazhar, M. (2014). Aerosol assisted chemical vapour deposited (AACVD) of TiO₂ thin film as compact layer for dye-sensitized solar cell. *Ceramics International*, 40(6), 8045-8052.
- Lindström, H., Holmberg, A., Magnusson, E., Malmqvist, L., & Hagfeldt, A. (2001). A new method to make dye-sensitized nanocrystalline solar cells at room temperature. *Journal of Photochemistry and Photobiology A: chemistry*, 145(1), 107-112.
- Liu, B., & Aydil, E. S. (2009). Growth of oriented single-crystalline rutile TiO₂ nanorods on transparent conducting substrates for dye-sensitized solar cells. *Journal of the American Chemical Society*, 131(11), 3985-3990.
- Lloyd Hughes, J., & Jeon, T. I. (2012). A review of the terahertz conductivity of bulk and nano-materials. *Journal of Infrared, Millimeter, and Terahertz Waves*, 33(9), 871-925.
- Martinson, A. B., Elam, J. W., Hupp, J. T., & Pellin, M. J. (2007). ZnO nanotube based dye-sensitized solar cells. *Nano letters*, 7(8), 2183-2187.
- Martinson, A. B., Hamann, T. W., Pellin, M. J., & Hupp, J. T. (2008). New architectures for dye-sensitized solar cells. *Chemistry*, 14(15), 4458-4467.
- Mathew, S., Yella, A., Gao, P., Humphry Baker, R., Curchod Basile, F. E., Ashari Astani, N., Tavernelli, I., Rothlisberger, U., Nazeeruddin Md, K., & Grätzel, M.

- (2014). Dye-sensitized solar cells with 13% efficiency achieved through the molecular engineering of porphyrin sensitizers. *Nat Chem*, 6(3), 242-247.
- Mikula, M., Gemeiner, P., Beková, Z., Dvonka, V., & Búc, D. (2015). Dye-sensitized solar cells based on different nano-oxides on plastic PET substrate. *Journal of Physics and Chemistry of Solids*, 76, 17-21.
- Mincuzzi, G., Vesce, L., Schulz Ruhtenberg, M., Gehlen, E., Reale, A., Di Carlo, A., & Brown, T. M. (2014). Taking Temperature Processing Out of Dye- Sensitized Solar Cell Fabrication: Fully Laser- Manufactured Devices. *Advanced Energy Materials*, 4(14).
- Mishra, A., Fischer, M. K., & Bäuerle, P. (2009). Metal- free organic dyes for dye-sensitized solar cells: From structure: Property relationships to design rules. *Angewandte Chemie International Edition*, 48(14), 2474-2499.
- Miyasaka, T., & Kijitori, Y. (2004). Low-temperature fabrication of dye-sensitized plastic electrodes by electrophoretic preparation of mesoporous TiO₂ layers. *J. Electrochem. Soc.*, 151(11), A1767-A1773.
- Moia, D., Vaissier, V., López-Duarte, I., Torres, T., Nazeeruddin, M. K., O'Regan, B. C., Nelson, J., & Barnes, P. R. (2014). The reorganization energy of intermolecular hole hopping between dyes anchored to surfaces. *Chemical Science*, 5(1), 281-290.
- Muliani, L., Hidayat, J., & Anggraini, P. N. (2016). *Performance analysis of flexible DSSC with binder addition*. Paper presented at the AIP Conference Proceedings.
- Ng, C. H., Lim, H. N., Hayase, S., Harrison, I., Pandikumar, A., & Huang, N. M. (2015). Potential active materials for photo-supercapacitor: A review. *Journal of Power Sources*, 296, 169-185.
- Nowotny, M. K., Bogdanoff, P., Dittrich, T., Fiechter, S., Fujishima, A., & Tributsch, H. (2010). Observations of p-type semiconductivity in titanium dioxide at room temperature. *Materials Letters*, 64(8), 928-930. doi: 10.1016/j.matlet.2010.01.061
- Pandikumar, A., Lim, S.-P., Jayabal, S., Huang, N. M., Lim, H. N., & Ramaraj, R. (2016). Titania@ gold plasmonic nanoarchitectures: An ideal photoanode for dye-sensitized solar cells. *Renewable and Sustainable Energy Reviews*, 60, 408-420.
- Peiris, T. N., Wijayantha, K. U., & García-Cañadas, J. (2014). Insights into mechanical compression and the enhancement in performance by Mg (OH) 2 coating in flexible dye sensitized solar cells. *Physical Chemistry Chemical Physics*, 16(7), 2912-2919.
- Qi, J., Xiong, H., Zhang, J., Zhang, Q., Li, Y., & Wang, H. (2017). Effects of release agents on the film morphology of TiO₂ photoanodes for FDSSCs by the roll-to-roll method. *Journal of Alloys and Compounds*, 702, 366-371.
- Ramasamy, E., Lee, W. J., Lee, D. Y., & Song, J. S. (2007). Nanocarbon counterelectrode for dye sensitized solar cells. *Applied Physics Letters*, 90(17), 173103.
- Roy Mayhew, J. D., & Aksay, I. A. (2014). Graphene materials and their use in dye-sensitized solar cells. *Chemical reviews*, 114(12), 6323-6348.
- Sönmezoğlu, S., Akyürek, C., & Akin, S. (2012). High-efficiency dye-sensitized solar cells using ferrocene-based electrolytes and natural photosensitizers. *Journal of Physics D: Applied Physics*, 45(42), 425101.
- Tang, K., Yu, X., Sun, J., Li, H., & Huang, X. (2011). Kinetic analysis on LiFePO₄ thin films by CV, GITT, and EIS. *Electrochimica Acta*, 56(13), 4869-4875.

- Temmer, R., Must, I., Kaasik, F., Aabloo, A., & Tamm, T. (2012). Combined chemical and electrochemical synthesis methods for metal-free polypyrrole actuators. *Sensors and Actuators B: Chemical*, 166, 411-418.
- Vivero-Escoto, J. L., Chiang, Y. D., Wu, K., & Yamauchi, Y. (2012). Recent progress in mesoporous titania materials: adjusting morphology for innovative applications. *Science and technology of advanced materials*, 13(1), 013003.
- Wang, Q., Moser, J.-E., & Grätzel, M. (2005). Electrochemical impedance spectroscopic analysis of dye-sensitized solar cells. *The Journal of Physical Chemistry B*, 109(31), 14945-14953.
- Weerasinghe, H. C., Huang, F., & Cheng, Y. B. (2013). Fabrication of flexible dye sensitized solar cells on plastic substrates. *Nano Energy*, 2(2), 174-189.
- Weerasinghe, H. C., Sirimanne, P. M., Simon, G. P., & Cheng, Y. B. (2012). Cold isostatic pressing technique for producing highly efficient flexible dye-sensitized solar cells on plastic substrates. *Progress in Photovoltaics: Research and Applications*, 20(3), 321-332.
- Wei, D., Unalan, H. E., Han, D., Zhang, Q., Niu, L., Amaratunga, G., & Ryhanen, T. (2008). A solid-state dye-sensitized solar cell based on a novel ionic liquid gel and ZnO nanoparticles on a flexible polymer substrate. *Nanotechnology*, 19(42), 424006.
- Wu, J., Hao, S., Lan, Z., Lin, J., Huang, M., Huang, Y., Li, P., Yin, S., & Sato, T. (2008). An all-solid-state dye-sensitized solar cell-based poly (N-alkyl-4-vinyl-pyridine iodide) electrolyte with efficiency of 5.64%. *Journal of the American Chemical Society*, 130(35), 11568-11569.
- Wu, J. H., Lan, Z., Lin, J. M., Huang, M., Hao, S., Sato, T., & Yin, S. (2007). A Novel Thermosetting Gel Electrolyte for Stable Quasi- Solid- State Dye- Sensitized Solar Cells. *Advanced Materials*, 19(22), 4006-4011.
- Wu, X., Lu, G. Q. M., & Wang, L. (2011). Shell-in-shell TiO₂ hollow spheres synthesized by one-pot hydrothermal method for dye-sensitized solar cell application. *Energy & Environmental Science*, 4(9), 3565-3572.
- Xiong, P., Huang, H., & Wang, X. (2014). Design and synthesis of ternary cobalt ferrite/graphene/polyaniline hierarchical nanocomposites for high-performance supercapacitors. *Journal of Power Sources*, 245, 937-946.
- Yang, J., Ganesan, P., Teuscher, J., Moehl, T., Kim, Y. J., Yi, C., Comte, P., Pei, K., Holcombe, T. W., & Nazeeruddin, M. K. (2014). Influence of the donor size in D- π -A organic dyes for dye-sensitized solar cells. *Journal of the American Chemical Society*, 136(15), 5722-5730.
- Yella, A., Lee, H. W., Tsao, H. N., Yi, C., Chandiran, A. K., Nazeeruddin, M. K., Diau, E. W. G., Yeh, C. Y., Zakeeruddin, S. M., & Grätzel, M. (2011). Porphyrin-sensitized solar cells with cobalt (II/III)-based redox electrolyte exceed 12 percent efficiency. *science*, 334(6056), 629-634.
- Yun, S., Freitas, J. N., Nogueira, A. F., Wang, Y., Ahmad, S., & Wang, Z.-S. (2016). Dye-sensitized solar cells employing polymers. *Progress in Polymer Science*, 59, 1-40.
- Zeng, Q., Yu, Y., Wu, L., Qi, B., & Zhi, J. (2010). Low- temperature fabrication of flexible TiO₂ electrode for dye- sensitized solar cells. *physica status solidi (a)*, 207(9), 2201-2206.
- Zhang, D., Yoshida, T., Furuta, K., & Minoura, H. (2004). Hydrothermal preparation of porous nano-crystalline TiO₂ electrodes for flexible solar cells. *Journal of Photochemistry and Photobiology A: chemistry*, 164(1), 159-166.
- Zhang, D., Yoshida, T., Oekermann, T., Furuta, K., & Minoura, H. (2006). Room-Temperature Synthesis of Porous Nanoparticulate TiO₂ Films for Flexible

- Dye- Sensitized Solar Cells. *Advanced Functional Materials*, 16(9), 1228-1234.
- Zhang, D. W., Li, X. D., Li, H. B., Chen, S., Sun, Z., Yin, X. J., & Huang, S. M. (2011). Graphene-based counter electrode for dye-sensitized solar cells. *Carbon*, 49(15), 5382-5388.
- Zhang, S., Yang, X., Numata, Y., & Han, L. (2013). Highly efficient dye-sensitized solar cells: progress and future challenges. *Energy & Environmental Science*, 6(5), 1443-1464.
- Zhao, L., Yu, J., Fan, J., Zhai, P., & Wang, S. (2009). Dye-sensitized solar cells based on ordered titanate nanotube films fabricated by electrophoretic deposition method. *Electrochemistry Communications*, 11(10), 2052-2055.
- Zubir, M. N. M., Badarudin, A., Kazi, S., Huang, N. M., Misran, M., Sadeghinezhad, E., Mehrali, M., & Yusoff, N. (2015). Highly dispersed reduced graphene oxide and its hybrid complexes as effective additives for improving thermophysical property of heat transfer fluid. *International Journal of Heat and Mass Transfer*, 87, 284-294.